Acenaphtho[5,6-*cd*]-1,2-dichalcogenoles and their Platinum Complexes

Louise M. Diamond, Fergus R. Knight, David B. Cordes, Andrew C. C. Ward, Alexandra M. Z. Slawin and J. Derek Woollins*

EaStCHEM, School of Chemistry, University of St Andrews, St Andrews, Fife, KY16 9ST (UK)
Fax: (+44)1334-463384
E-mail: jdw3@st-and.ac.uk

Keywords: Chalcogen / Acenaphthylene / Platinum / Metathesis / X-ray Structure/ Coordination complex

Abstract

A related series of *bis*(phosphine) platinum complexes **1**-**5** and **6**-**8** bearing dichalcogenate acenaphthylene ligands have been synthesised. The chalcogen-chalcogen bonds in the parent acenaphtho[5,6-*cd*]-1,2-dichalcogenoles (AcenapylE_2; **L1** E = S, **L2** E = Se; Acenapyl = acenaphthylene-5,6-diyl) were reduced with two equivalents of lithium triethylborohydride to form the dilithio-species. Metathetical addition of the lithium dichalcogenate species to a suspension of the appropriate *cis*-dichloro*bis*(phosphine)platinum in THF resulted in the formation of platinum (II) complexes [Pt(5,6-AcenapylE_2)(PR_3)$_2$] (**1** E = S, R_3 = Ph_3; **2** E = S, R_3 = Ph_2Me; **3** E = S, R_3 = $PhMe_2$; **4** E = S, R_3 = Me_3; **6** E = Se, R_3 = Ph_3; **7** E = Se, R_3 = Ph_2Me; **8** E = Se, R_3 = $PhMe_2$). The dilithio-species of **L1** and **L2** were also reacted with (1,5-cyclooctadiene)platinum(II) dichloride. This reaction was successful with **L1** resulting in the formation of platinum complex [Pt(5,6-AcenapylS_2)(COD)] (**5**). Complexes **1**-**3** and **5**-**8** have been fully characterised, principally by multinuclear magnetic resonance spectroscopy, IR and MS. Secondary isotopomer effects create complex satellite systems observed in both the $^{31}P\{^1H\}$ NMR and ^{77}Se NMR spectra of selenium complexes **6**-**8**. X-ray structures were determined for **L1**, **1**, **3** and **6** and analysed, where appropriate, by measuring the *peri*-distance, splay angle magnitude, *peri*-atom displacement, central naphthalene ring torsions and the geometry around the platinum centre. Platinum was found to adopt a distorted square-planar geometry in all three complexes. Complex **1** was found to have the greatest molecular distortion of all three complexes, showing that changing the phosphine group and also the chalcogen has a noticeable effect. Comparisons were made between **6** and our previously reported [Pt(NapSe_2)(PPh_3)$_2$] and [Pt(AcenapSe_2)(PPh_3)$_2$] complexes; the level of distortion was found to decrease as the backbone is altered from naphthalene to acenaphthylene.

Introduction

The family of polycyclic aromatic hydrocarbons naphthalene, acenaphthene and acenaphthylene offer suitable rigid organic backbones with which to study non-bonded intramolecular interactions.[1,2,3] Heteroatoms that are substituted at the *peri*-positions in these systems (positions 1- and 8- of the naphthalene ring and positions 5- and 6- of the acenaphthene and acenaphthylene rings) are forced to occupy space that is closer than the sum of their van der Waals radii, allowing unique interactions to transpire between the bulky substituents. Hydrogen atoms can be accommodated in the *peri*-positions with ease because the non-bonded hydrogen distances in naphthalene, acenaphthene and acenaphthylene (2.44 Å, 2.70 Å, 2.73 Å)[1,2,3] are still greater than the sum of the van der Waals radii for two hydrogen atoms (Σr_{vdw} = 2.18 Å).[4] If these *peri*-hydrogens are replaced with larger substituents though, steric hindrance is expected as there is not enough space for the larger groups to be accommodated without a significant overlap of orbitals.[5] Despite this, a great array of *peri*-substituted

naphthalenes[6] have been prepared due to the system's ability to relieve strain through the deformation of the organic framework or by the existence of attractive interactions operating between the two substituents. While some *peri*-substituted acenaphthenes[7] and acenaphthylenes[8] have been prepared they have received much less attention than naphthalene systems.[6]

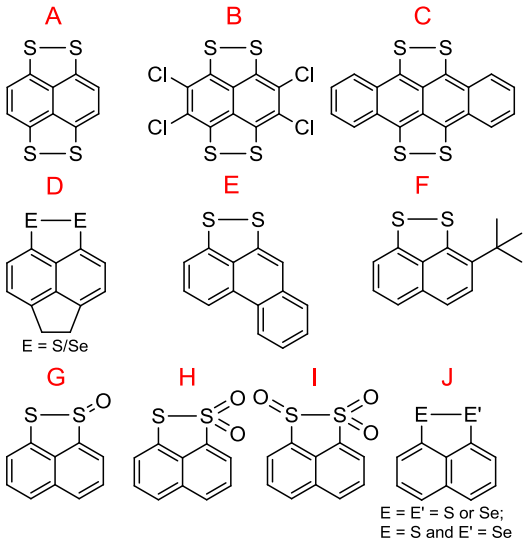

Figure 1. *Peri*-substituted dichalcogenole ligands previously utilised in the formation of platinum complexes.[9,10,11]

In the late 1970's and early 1980's Teo and co-workers[9] coordinated tetrathionaphthalene (TTN; Figure 1 A), tetrachloro-tetrathionaphthalene (TCTTN; B) and tetrathiotetracene (TTT; C) to a $Pt(PPh_3)_2$ centre through oxidative addition reactions with $[Pt(PPh_3)_4]$. Due to the structural similarity of these compounds to naphthalene, we used this oxidative reaction to study the coordination chemistry of 1,8-dichalcogen naphthalenes and related species to platinum *bis*phosphines.[10] The acenaphthene (D), phenanthrene (E), 2-*tert*-butyl-substituted naphthalene dithiolate (F) and the oxides of naphtho[1,8-*cd*]-1,2-dithiole (G-I) (with the exception of the tetra oxide) were successfully complexed to platinum through oxidative addition of $[Pt(PPh_3)_4]$.[10] The naphtho[1,8-*cd*][1,2]dithiole, naphtho[1,8-*cd*][1,2]diselenole and naphtho[1,8-*cd*][1,2]selanthiole platinum complexes were also prepared through a metathetical reaction of the dilithio-1,8-dichalcogenato naphthalene (J), but with *cis*-$[Pt(PR_3)_2Cl_2]$ (where R = Ph or Me) in THF at room temperature.[10]

We furthered this study in 2013 by preparing and fully characterising six platinum *bis*(phosphine) complexes constructed from 5,6-dihydroacenaphtho[5,6-*cd*]-1,2-dithiole [$AcenapS_2$] and 5,6-dihydroacenaphtho[5,6-*cd*]-1,2-diselenole [$AcenapSe_2$] (D).[11] These complexes were prepared through metathetical reaction of the dilithio salt of the parent acenaphthene, with a suspension of *cis*-$[Pt(PR_3)_2Cl_2]$ (where R = Ph_3, Ph_2Me, $PhMe_2$). Herein we build on the aforementioned studies through the preparation and structural analysis of seven analogous acenaphthylene based platinum *bis*phosphine complexes $[Pt(5,6\text{-}AcenapylE_2)(PR_3)_2]$ (R_3 = Ph_3: E = S **1**, Se **6**; R_3 = Ph_2Me: E = S **2**, Se **7**; R_3 = $PhMe_2$: E = S **3**, Se **8**; R_3 = Me_3: E = S **4**; Acenapyl = acenaphthylene-5,6-diyl) formed by metathetical methods from acenaphtho[5,6-*cd*]-1,2-dichalcogenoles [$AcenapylE_2$] (**L1** E = S, **L2** E = Se) and *cis*-$[PtCl_2(PR_3)_2]$ (R_3 = Ph_3, Ph_2Me, $PhMe_2$, Me_3; Scheme 2).

Results and Discussion

Platinum *bis*(phosphine) complexes **1-4** and **6-8** bearing acenaphtho[5,6-*cd*]-1,2-dichalcogenoles [$AcenapylE_2$] (**L1** E = S, **L2** E = Se) have been prepared by metathesis from *cis*-$[PtCl_2(PR_3)_2]$ (R_3 = Ph_3, Ph_2Me, $PhMe_2$, Me_3) and the dilithium salts

of the parent dichalcogen acenaphthylene ligands in 22-48% yield. The platinum complex [Pt(COD)**L1**] (**5**) was also prepared from (1,5-cyclooctadiene)platinum(II) dichloride. Ligands **L1** and **L2** and complexes **1**-**3** and **5**-**8** were synthesised and fully characterised, principally by multinuclear magnetic resonance, IR spectroscopy and mass spectrometry. The homogeneity of the new compounds was, where possible, confirmed by microanalysis.

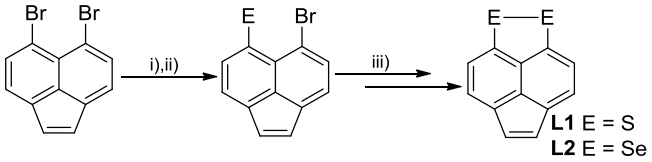

Scheme 1. Synthetic route to AcenapylS_2 (**L1**) and AcenapylSe_2 (**L2**): i) TMEDA (2 eq.), *n*BuLi (1 eq.), THF, -78 °C, 30 min; ii) E (1 eq.), THF, -40 °C, 2 h; iii) TMEDA (2 eq.), *n*BuLi (1 eq.), THF, -78 °C, 30 min then E (1 eq.), THF, -40 °C.

The ligands acenaphtho[5,6-*cd*]-1,2-dithiole (AcenapylS_2, **L1**) and acenaphtho[5,6-*cd*]-1,2-diselenole (AcenapylSe_2, **L2**) were prepared following a modification of the literature procedure (Scheme 1).[12] Two equivalents of TMEDA were added to a solution of 5,6-dibromoacenaphthylene[13] in diethyl ether at -78 °C. One equivalent of *n*BuLi was added dropwise and the solution was left to stir for fifteen minutes. One equivalent of the appropriate chalcogen was added, the temperature was raised to -40 °C and the reaction left to stir for two hours. A further one equivalent of *n*BuLi and chalcogen were added to replace the remaining bromine and then a further equivalent of chalcogen was added. After mild oxidation in air and purification the dichalcogen bridged ligands **L1** and **L2** were collected in yields of 5% and 26%, respectively. Attempts to improve these yields proved unsuccessful.

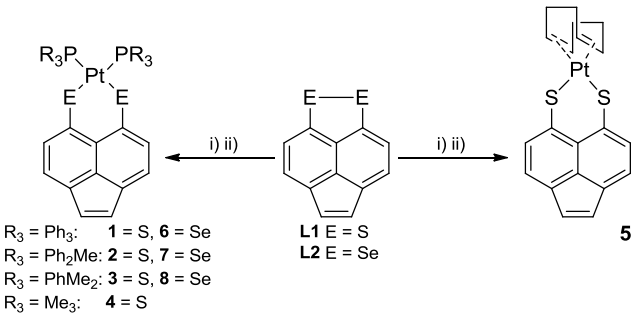

Scheme 2. Reaction route for the synthesis of the platinum (II) complexes [Pt(5,6-AcenapylE_2)(PR_3)$_2$] **1**-**4**, **6**-**8** and [Pt(COD)**L1**] **5**: i) LiBEt_3H (2 eq.), THF, r.t.; ii) [$PtCl_2$(PR_3)$_2$]/[Pt(COD)Cl_2], THF.

Synthesis of the platinum complexes followed a metathetical reaction that has been well documented in the preparation of similar complexes (Scheme 2).[9,10,11] The chalcogen-chalcogen bonds in **L1** and **L2** were reduced with two equivalents of lithium triethylborohydride in tetrahydrofuran at room temperature to form the dilithio-species. Metathetical addition of the dilithio-species to a suspension of the appropriate *cis*-dichloro*bis*(phosphine)platinum in tetrahydrofuran resulted in the formation of the platinum complexes [Pt(5,6-AcenapylE_2)(PR_3)$_2$] (R_3 = Ph_3: E = S **1**, Se **6**; R_3 = Ph_2Me: E = S **2**, Se **7**; R_3 = $PhMe_2$: E = S **3**, Se **8**; R_3 = Me_3: E = S **4**). ^{31}P NMR stiudies of the cryde reaction mixtures showed only starting material and product resonances Unfortunately, despite changing conditions and several different attempts the yields were not improved and complex **4** was obtained in poor yield and only ^{31}P NMR was acquired. The dilithio-species of **L1** and **L2** were also reacted with (1,5-cyclooctadiene)platinum(II) dichloride. This reaction was successful with **L1** resulting in the platinum complex [Pt(5,6-AcenapylS_2)(COD)] (**5**) (Scheme 2).

Table 1. $^{31}P\{^{1}H\}$ NMR spectroscopic data for complexes **1**-**4**, **6**-**8**.

	Chemical Shifts [ppm]	Coupling Constants [Hz]
Product	$\delta(^{31}P)$	$^{1}J(^{31}P\text{-}^{195}Pt)$
1	23.9	2953
2	3.5	2880
3	-14.5	2819
4	-24.7	2768

	Chemical Shifts [ppm]	Coupling Constants [Hz]	
Product	$\delta(^{31}P)$	$^{1}J(^{31}P\text{-}^{195}Pt)$	$^{2}J(^{31}P\text{-}^{77}Se)$
6	20.2	3014	54
7	0.6	2932	54
8	-17.6	2873	52

$^{31}P\{^{1}H\}$ NMR spectroscopic data for the series of *bis*phoshine complexes is displayed in Table 1. The spectra of complexes **1**-**4**, bearing the sulfur ligand **L1**, display the expected single resonances with platinum satellites. As the alkyl groups on phosphorus are varied from R_3= Ph_3 to R_3=Me_3 the resonance peak moves to a lower chemical shift [**1** δ = 23.9 ppm, $^{1}J(^{31}P,^{195}Pt)$ = 2953 Hz; **2** δ = 3.5 ppm, $^{1}J(^{31}P,^{195}Pt)$ = 2880 Hz; **3** δ = -14.5 ppm $^{1}J(^{31}P,^{195}Pt)$ = 2819 Hz; **4** δ = -24.7 ppm, $^{1}J(^{31}P,^{195}Pt)$ = 2768 Hz], this trend was also observed in the analogous acenaphthene compounds.[11] Previously it has been observed that higher $^{1}J(^{31}P\text{-}^{195}Pt)$ coupling constants exist for more electron withdrawing R groups, with $^{1}J(^{31}P\text{-}^{195}Pt)$ decreasing as phenyl groups are replaced with electron donating methyl groups.[10,11] It can be seen for **1**-**4** that there is a steady decrease in value for $^{1}J(^{31}P\text{-}^{195}Pt)$ coupling as phenyl groups are replaced by more electron donating methyl groups. An equivalent trend is observed in the corresponding $^{31}P\{^{1}H\}$ NMR spectra of complexes **6**-**8**, which similarly display single resonances with platinum satellites at **6** $\delta(^{31}P)$ = 20.2 ppm ($^{1}J(^{31}P,^{125}Pt)$ = 3014 Hz), **7** $\delta(^{31}P)$ = 0.60 ppm ($^{1}J(^{31}P,^{125}Pt)$ = 2932 Hz) and **8** $\delta(^{31}P)$ = -17.6 ppm ($^{1}J(^{31}P,^{125}Pt)$ = 2873 Hz) respectively, but with additional satellites attributed to $^{31}P\text{-}^{77}Se$ coupling ($^{2}J(^{31}P,^{77}Se)$ = **6** 54 Hz, **7** 54 Hz, **8** 52 Hz). The same pattern was observed in the $^{31}P\{^{1}H\}$ NMR spectrum of analogous naphthalene complex [Pt($NapSe_2$)(PPh_3)$_2$] ($\delta(^{31}P)$ = 20.5 ppm ($^{1}J(^{31}P,^{125}Pt)$ = 3016 Hz, $^{2}J(^{31}P,^{77}Se)$ = 51Hz).[10]

In symmetrical systems such as these, the presence of the NMR-inactive isotopomer at the second Se coordination site causes the two ^{31}P environments to become magnetically inequivalent due to the resulting break in symmetry of the molecule. Consequently, each ^{31}P atom can align either *cis* or *trans* to the low abundance ^{77}Se NMR active isotope (7.6%),[14] which can result in two distinct, but comparable $^{31}P\text{-}^{77}Se$ coupling values. This secondary isotopomer effect was observed in the spectra of previously reported naphthalene [Pt($NapSe_2$)(PMe_3)$_2$] and acenaphthene [Pt($AcenapSe_2$)($PPhMe_2$)$_2$] platinum complexes with $^{2}J_{PSe}$ coupling observed for both the *cis* (47 Hz, 47 Hz) and *trans* (53 Hz, 56 Hz) configurations in each case (Figure 2).[10,11] The absence of two distinct sets of satellites for *cis*/*trans* $^{2}J(^{31}P,^{77}Se)$ coupling in the $^{31}P\{^{1}H\}$ NMR spectra of complexes **6**-**8** suggests the coupling constants are of a similar magnitude, and the individual satellites overlap; this is confirmed by measuring integral peak intensities (^{31}P:^{77}Se). In addition, $^{1}J(^{31}P,^{31}P)$ coupling constants are notoriously small in such AA`X spin systems[15**]** and as such are also not observed in $^{31}P\{^{1}H\}$ NMR spectra of complexes **6**-**8**.

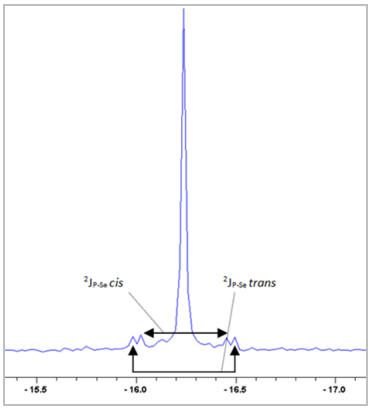

Figure 2. $^{31}P\{^1H\}$ NMR spectrum for [Pt(AcenapSe$_2$)(PPhMe$_2$)$_2$] showing the *cis* and *trans* satellites with $^2J_{PSe}$ coupling.[11]

Unsurprisingly, secondary isotopomer effects are also observed in the ^{77}Se NMR spectra of **6**-**8** which display complex satellite systems due to *cis*/*trans* $^2J(^{77}Se,^{31}P)$ coupling and $^1J(^{77}Se,^{195}Pt)$ coupling. The spectra of complexes **6** and **7** are poorly resolved and appear as approximate 'septets' centred at $\delta(^{77}Se)$ = 228 ppm and $\delta(^{77}Se)$ = 204 ppm, respectively. The ^{77}Se NMR resonance of complex **8**, meanwhile, appears as an overlapping second-order doublet of doublets centred at $\delta(^{77}Se)$ = 174.6 ppm, with *cis* and *trans* $^2J(^{77}Se,^{31}P)$ coupling ≈ 52 Hz and reciprocal satellites for $^1J(^{77}Se,^{195}Pt)$ coupling (251 Hz; Figure 3). The values seen for the $^1J_{SePt}$ satellites are similar to those observed by other groups.[16]

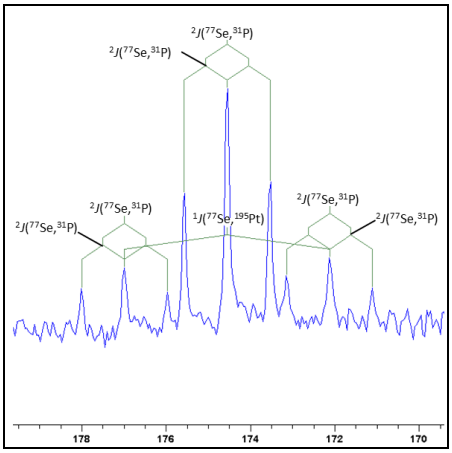

Figure 3. ^{77}Se NMR spectrum for complex **8** displaying the overlapping second-order doublet of doublets and corresponding ^{195}Pt satellites.

As previously discussed, a steady decrease in magnitude is observed in the $^1J(^{31}P\text{-}^{195}Pt)$ coupling constant as the phenyl groups are replaced by methyl groups (Table 1). In contrast, a steady increase in magnitude is observed in the $^1J(^{77}Se\text{-}^{195}Pt)$ coupling constant. These opposing trends are due to a combination of factors. A decrease in electronegativity of the alkyl groups occurs each time a phenyl is replaced by a methyl. The platinum centre becomes more electron rich as a consequence of the alkyl groups becoming more electropositive, this causes a decrease in the *s*-character of the P-Pt bond. This implies the lone pair on the phosphorus is less tightly bound and subsequently strengthens the P-Pt bond. The *s*-character of the P-Pt

bond decreases because the platinum becomes more electron rich as methyl groups are added, in turn the P-C_R bond adopts more *s*-character to stabilise the local negative charge.[17]

In addition, the increase in $^{1}J(^{77}Se\text{-}^{195}Pt)$ coupling constants can be partially attributed to phenyl groups being greater π-acceptors than methyl groups. When π-acceptors are in the *trans* position they reduce the magnitude of the coupling constant between the metal and the ligand i.e. platinum and selenium. As phenyl is replaced with the poorer π-acceptor methyl the coupling constant increases. However, the *trans* influence is not fully responsible for the increase we observe in coupling constant, the *s*-character in the Pt-Se bond and the subsequent *s*-electron density at the platinum centre is also responsible.[17]

Table 2. Selected interatomic distances [Å] and angles [°] for **L1**, **1**, **3**, **6**.

Compound	**L1**	**1**	**3**	**6**
Ligand; *peri*-atoms	SS	**L1**; SS	**L1**; SS	**L2**, SeSe
E(1)···E(2)	2.084(2)	3.343(3)	3.431(11)	3.452(4)
Σr_{vdW} – E(1)···E(2)[a]; % Σr_{vdW} [a]	1.516; 58	0.257; 93	0.169; 95	0.348; 91
Peri-region bond angles				
E(1)-C(1)-C(10)	113.88(16)	124.6(6)	127(3)	127.8(7)
C(1)-C(10)-C(9)	118.78(16)	128.8(7)	131(3)	131.0(8)
E(2)-C(9)-C(10)	115.66(16)	127.1(6)	128(2)	127.4(7)
Σ of bay angles	348.32(28)	380.5(11)	386(5)	386.2(13)
Splay angle[b]	-11.7	20.5	26.0	26.2
Out-of-plane displacement				
E(1)	0.090(1)	-0.525(1)	-0.009(1)	0.012(1)
E(2)	0.020(1)	0.449(1)	0.105(1)	-0.019(1)
Central naphthalene ring torsion angles				
C:(6)-(5)-(10)-(1)	178.12(15)	-172.7(7)	179(3)	-179.2(9)
C:(4)-(5)-(10)-(9)	-177.80(16)	-177.7(7)	-174(3)	178.7(9)

[a] van der Waals radii used for calculations: r_{vdW}(S) 1.80 Å, r_{vdW}(Se) 1.90 Å[4]; [b] Splay angle: Σ of the three bay region angles – 360.

X-ray Investigations: Single crystals were obtained for **L1** by cooling a hot hexane solution to -35 °C overnight. The molecular structure of **L1** is shown in Figure 5. Although **L1** is a known compound with published characterisation data,[12] no crystal data have been published. The crystal structure of **L1** has a *peri* sulfur-sulfur bond distance of 2.084(2) Å. This is much shorter than the *peri*-distance in unsubstituted acenaphthylene of *ca.* 2.73 Å,[3] this is expected as a bond has formed between the *peri*-substituents. However, the S-S bond does fall within the 'normal' length for a compound of this type with typical values of *ca.* 2.05 Å being reported.[18] The *peri*-angles in acenaphthylene are 120.3(8)°, 127.8(6)° and 120.3(8)° with the sum being 368.4°.[3] In **L1** the sum of the bay angles is 348.32(28)° with a resulting negative splay angle of -11.7°; this is less than the sum in ideal acenaphthylene confirming a favourable interaction is occurring between the *peri*-atoms resulting in the formation of a *peri*-bond. Minor out-of-plane distortion is observed with both sulfur atoms sitting 0.02(1) Å and 0.09(1) Å away from the naphthyl plane. This is accompanied by a minor distortion to the geometry of the 'naphthalene' framework with C-C-C-C torsion angles deviating by 1.88° and 2.20° from the 'ideal' 180°.

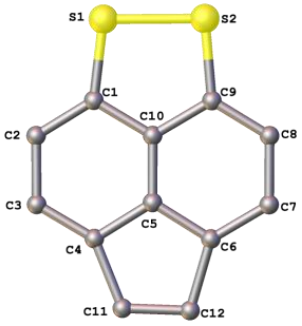

Figure 5. The molecular structure of **L1** with H atoms omitted for clarity.

It is not surprising that **L1** displays similar characteristics to naphtha[1,8-*cd*][1,2]dithiole [$NapS_2$][10] and 5,6-dihydroacenaphtho[5,6-*cd*]-1,2-dithiole [$AcenapS_2$].[11] The *peri*-distances observed in all three compounds are statistically equivalent with values of 2.0879(8) Å,[10] 2.1025(19) Å[11] and 2.084(2) Å for $NapS_2$, $AcenapS_2$ and **L1**, respectively. The C(4)-C(5)-C(6) angle in $NapS_2$ is 125°,[10] the addition of the ethane/ethene bridge in $AcenapS_2$/**L1** causes compression of this angle, with values of 114.9(5)°[11] and 116.30(16)°, respectively. One would expect compression of the C(4)-C(5)-C(6) angle to cause an expansion in the C(1)-C(10)-C(9) angle however, this is not strictly the case. An increase in the C(1)-C(10)-C(9) angle is seen between $NapS_2$ and $AcenapS_2$ (118.65(16)° to 120.2(5)°),[10,11] but a decrease then occurs with **L1** having a C(1)-C(10)-C(9) angle of 118.78(16)°. This is reflected in the splay angles with values of -11.2°,[10] -11.8°[11] and -11.7° for $NapS_2$, $AcenapS_2$ and **L1**, respectively. All three ligands have similar out-of-plane displacement with the sulfur atoms sitting *ca.* 0.02 Å from the naphthyl plane. **L1** has the largest, although still minor, naphthalene framework distortion with C-C-C-C torsion angles deviating from 180° by 1.88° and 2.20° (*cf.* $NapS_2$ and $AcenapS_2$ *ca*. 0.40°).[10,11]

Single crystals were obtained for **1** by evaporation of a saturated solution of the compound in chloroform. **1** crystallises with two dichloromethane molecules per platinum molecule. Single crystals of **3** and **6** were obtained by diffusion of hexane into a saturated solution of the compound in diethyl ether. The molecular structures of **1**, **3** and **6** are shown in Figures 6 and 10, respectively.

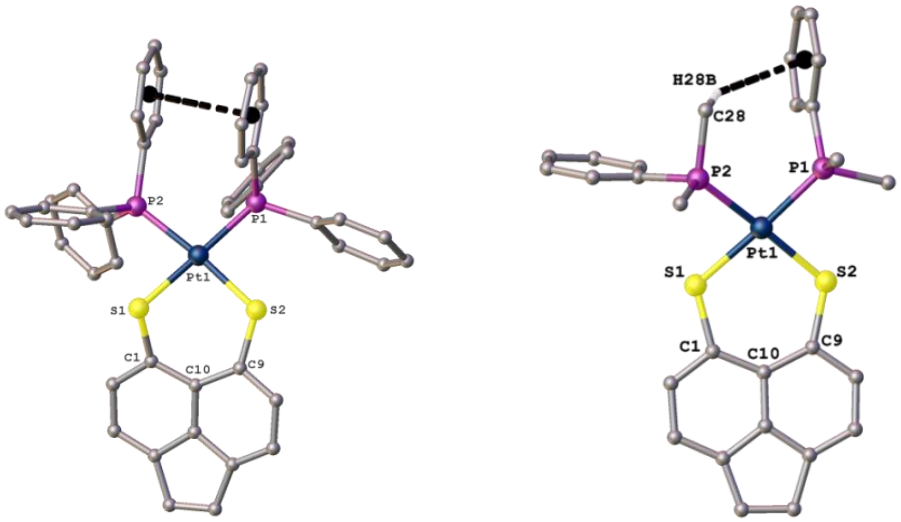

Figure 6. The molecular structures of **1** and **3**, showing the weak intramolecular interactions; solvent molecules and H atoms omitted for clarity.

Table 3. Platinum coordination geometry; selected intramolecular distances [Å] and angles [°] for **1**, **3**, and **6**.

Complex	**1**	**3**	**6**
Ligand; *peri*-atoms	**L1**; SS	**L1**, SS	**L2**, SeSe
Metal geometry – bond lengths			
E(1)-Pt(1)	2.326(2)	2.334(9)	2.432(2)
E(2)-Pt(1)	2.3212(19)	2.315(8)	2.4449(19)
P(1)-Pt(1)	2.289(2)	2.293(9)	2.305(3)
P(2)-Pt(1)	2.2991(19)	2.293(9)	2.290(3)
Metal geometry – bond angles			
E(1)-Pt(1)-E(2)	92.07(7)	95.1(3)	90.12(8)
P(1)-Pt(1)-P(2)	96.08(7)	93.6(3)	96.98(11)
E(1)-Pt(1)-P(2)	82.96(7)	83.9(3)	86.97(10)
E(2)-Pt(1)-P(1)	88.94(7)	87.5(3)	86.93(10)
Envelope geometry			
E_2C_3-Pt angle	144.13 (1)	154.79(1)	142.98(1)
E_2C_3-Pt distance	0.937(1)	0.576(1)	1.037(1)

In the three complexes, the dichalcogenate acenaphthylene acts as a bidentate ligand, coordinating to the platinum *via* the two chalcogen atoms to form a six-membered PtC_3E_2 chelate ring. A distorted square planar geometry is adopted by the platinum centre in each case, with angles deviating from the ideal (90°). As expected the *peri*-distances in **1** and **3** have been elongated due to the breaking of the sulfur-sulfur bond and insertion of the platinum. The non-bonded sulfur-sulfur distance being 3.343(3) Å for **1** and 3.431(11) Å for **3** compared to the bonded distance of 2.084(2) Å in the free ligand **L1**. However, the *peri*-distance in the two complexes is still shorter than the sum of the van der Waals radii for two sulfur atoms by 5-7%. The angles of the bay region increase as a consequence of the increase in *peri*-distance, with positive splay angles of 20.5° and 26.0° being seen for **1** and **3** respectively. This is significantly greater than the negative splay angle of -11.7° that is observed in **L1** due to the presence of the sulfur-sulfur bridge.

1 displays much greater distortion of the naphthalene skeleton than **3**. The non-bonded *peri*-distance and the splay angle in **3** are larger than those in **1** creating a more relaxed geometry around the platinum centre which can accommodate the dimethyl-phenylphosphine groups without causing great distortion to the naphthalene backbone. In **L1** the sulfur atoms lie 0.09(1) Å and 0.02(1) Å above the naphthyl plane. **1** displays significant out-of-plane distortion in comparison to the ligand; one sulfur atom sits 0.525(1) Å below the naphthyl plane and the other sits 0.449(1) Å above the plane. **3** shows less out-of-plane distortion than **1**, with one sulfur atom lying 0.105(1) Å above the naphthyl plane and the other lying on the plane. The torsion angles also deviate from the free ligand by *ca.* 1-7.3° with **1** showing the greatest buckling of the naphthalene carbon framework. Greater distortion is observed in **1** due to the bulky triphenylphosphine groups making it more difficult for the complex to maintain a square planar environment around the platinum centre when compared to the smaller dimethylphenylphosphine groups.

Changing the alkyl groups from triphenylphosphines to dimethylphenylphosphines has a minor effect on the geometry of the corresponding acenaphthene complexes, [Pt(AcenapS_2)(PPh_3)$_2$] and [Pt(AcenapS_2)($PPhMe_2$)$_2$].[11] Unfortunately a comparison with the equivalent naphthalene complexes is not possible, as [Pt(NapS_2)(PPh_3)$_2$] could not be crystallised and [Pt(NapS_2)($PPhMe_2$)$_2$] has not been prepared.[10]

In **1** a weak π···π interaction is observed with two phenyl rings, one from each PPh_3 group, adopting a face-to-face alignment (Figure 6) with a Cg(C13-C18)····Cg(C31-C36) distance of 3.620(1) Å. This value is comparable with that found in the acenaphthene complex [Pt(AcenapS_2)(Pt(PPh_3)$_2$] which has a Cg(C25-C30)····Cg(C31-C36) distance of 3.765(1) Å.[11] However, in **3** the intramolecular interaction observed is a C-H····π interaction, it is now a phenyl ring from one PPh_2Me group that is interacting with a methyl group from the other PPh_2Me group (Figure 6), giving a C28-H28B····Cg(C13-C18) distance of 2.847(1) Å. Again, this value is comparable with [Pt(AcenapS_2)($PPhMe_2$)$_2$] which has a C14-H14····Cg(C23-C28) distance of 2.61(1) Å.[11]

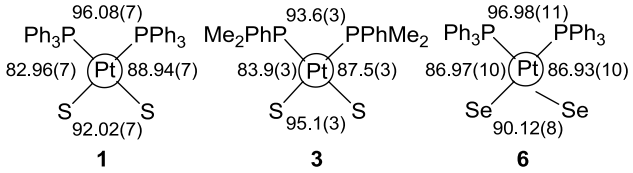

Figure 7. Comparison of the angles (°) associated with the square planar geometry of the platinum metal in complexes **1**, **3** and **6**.

The platinum metal centre in **1** and **3** maintains a distorted square planar geometry (Figure 7). The P(1)-Pt(1)-P(2) angle of 96.08(7)° for **1** is larger than the P(1)-Pt(1)-P(2) angle of 93.6(3)° in 3. This angle is larger in **1** in order to accommodate the bulky triphenylphosphine groups; replacement of two phenyl groups with the less sterically demanding methyl groups allows reduction of this angle to occur in **3**. One would expect the S(1)-Pt(1)-P(2) and S(2)-Pt(1)-P(1) angles to be equal, however this is not the case. This is a consequence of the distortion in the naphthalene framework. The P(1)-Pt(1)-P(2) angle in **1** is smaller than that in **3** (92.02(7)° and 95.1(3)°) this is expected as the *peri*-distance and splay angle observed in **3** is more relaxed than those in **1**. No significant differences in the Pt bond lengths are observed between the complexes.

In **1** and **3**, **L1** acts as a bidentate ligand, coordinating to the platinum *via* the chalcogen atoms to form a six-membered chelate ring. This six-membered PtS_2C_3 ring can be described as having a twisted envelope type conformation with the S···S vector as the hinge (Figure 8). In **1** C(1), C(10) and C(9) all lie in a plane with S(1) lying 0.525(1) Å below the plane and S(2) lying 0.449(1) Å above the plane. This results in a non-planar, twisted PtS_2C_3 ring. In **3** the PtS_2C_3 ring is closer to planar with the sulfur atoms deviating from the plane by 0.009(1) Å and 0.105(1) Å. The mean plane of S(1), S(2), C(1), C(10) and C(9) and the displacement of Pt(1), which sits in the *peri*-gap above the plane, is measured. In **1** the Pt(1) sits 0.937(1) Å above the mean plane and the angle of the S(1)···S(2) hinge is 144.13(1)°. Whereas in **3** the Pt(1) sits 0.576(1) Å above the mean plane and the S(1)···S(2) hinge angle is 154.79(1)°. The larger angle and in turn shorter Pt(1) displacement observed for **3** is expected due to this complex displaying less distortion than **1**.

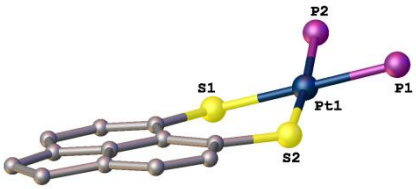

Figure 8. The twisted envelope configuration of the 6-membered chelate ring, formed from bidentate S coordination of **L1** in complex **3** (phenyl and methyl groups and H atoms omitted for clarity).

The non-bonded *peri*-distance in **1** of 3.343(3) Å is shorter than that of 3.452(4) Å in **6**. This is expected due to the van der Waals radius of sulfur being smaller than that of selenium (1.80 Å vs. 1.90 Å).[4] The *peri*-distance observed in both complexes is shorter than the sum of their respective van der Waals radii by 7-9%. As expected, breaking of the chalcogen-chalcogen *peri*-bond and insertion of the platinum results in a positive splay angle being observed in both complexes with **6** having a larger splay angle than **1** (26.2° and 20.5°). Significant out-of-plane distortion is observed in **1** with one sulfur atom lying 0.525(1) Å below the acenaphthylene plane and the other lying 0.449(1) Å above the plane (Figure 9). This is accompanied by distortion of the acenaphthylene ring with torsion angles deviating from the ideal 180° by 2.3-7.2°. In comparison, **6** shows much less distortion with the selenium atoms lying 0.012(1) Å and 0.019(1) Å above and below the acenaphthylene plane (Figure 9). The acenaphthylene ring shows little buckling with torsion angles varying from 180° by 0.8-1.3°. Similar trends in *peri*-distance and splay angle are seen between $[Pt(AcenapS_2)(PPh_3)_2]$ and $[Pt(AcenapSe_2)(PPh_3)_2]$. However, differences are observed in out-of-plane distortion and torsion angles with both acenaphthene complexes having similar values and therefore similar levels of distortion.[11]

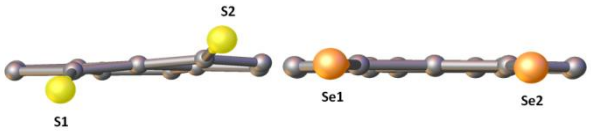

Figure 9. Comparison of the out-of-plane distortion and naphthalene ring deformation seen in **1** and **6**, other atoms have been omitted for clarity.

In **1** two phenyl rings, one from each of the two PPh_3 groups, adopt a face-to-face alignment leading to a weak π···π interaction (Figure 6) with a Cg(C13-C18)····Cg(C31-C36) distance of 3.620(1) Å. **6** also shows a weak π···π interaction (Figure 10) with a Cg(C13-C18)····Cg(C37-C42) distance of 3.801(1) Å. These values are comparable with those seen in $[Pt(AcenapS_2)(PPh_3)_2]$ (3.765(1) Å) and $[Pt(AcenapSe_2)(PPh_3)_2]$ (3.764(1) Å).[11]

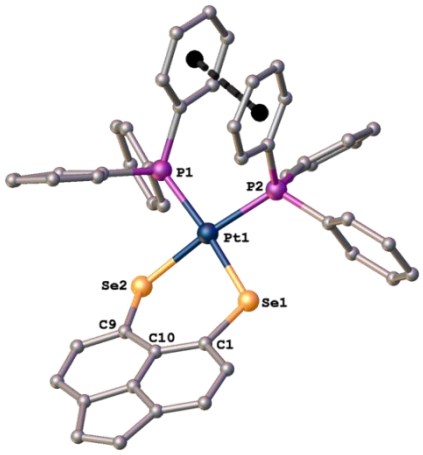

Figure 10. The molecular structures of **6**, showing the weak π···π interaction with H atoms omitted for clarity.

In **1** and **6** the platinum metal centre adopts a distorted square planar geometry (Figure 7). The P(1)-Pt(1)-P(2) angle of 96.08(7)° and 96.98(11)° for **1** and **6**, respectively is larger than the ideal 90° in order to accommodate the bulky triphenylphosphine groups. The E-Pt-P angles observed in both complexes are smaller than 90°, the expansion of the P(1)-Pt(1)-P(2) angle causes compression of these angles due to the restriction imposed by the *peri*-geometry which fixes the sulfur and selenium atoms. The Se(1)-Pt(1)-P(2) and Se(2)-Pt(1)-P(1) angles of 86.97(10)° and 86.93(10)° are equal. In comparison the S(1)-Pt(1)-P(2) angle of 82.96(7)° is much smaller than the S(2)-Pt(1)-P(1) angle of 88.94(7)°, this is due to the large out-of-plane distortion of the sulfur atoms causing twisting in the PtS_2C_3 ring. The S(1)-Pt(1)-S(2) angle of 92.02(7)° is larger than the Se(1)-Pt(1)-Se(2) of 90.12(8)°. One would expect the S(1)-Pt(1)-S(2) to be the smaller angle as the non-bonded *peri*-distance observed in **1** is smaller than that of **6** (3.343(3) Å and 3.452(4) Å, respectively). However, the out-of-plane distortion in **1** is much greater than that in **6**, as a consequence of this the most comfortable position for the sulfur atoms to sit results in a larger angle than that of the selenium atoms. No significant differences in the Pt-P bond lengths are observed between the complexes; however there are differences in the Pt-E bond lengths. The Pt-Se bond lengths of 2.432(2) Å and 2.4449(19) Å are longer than the Pt-S bond lengths of 2.326(2) Å and 2.3212(19) Å.

As previously discussed for **1** and **3** the six-membered PtE_2C_3 chelate ring, that forms when the dichalcogenate ligand binds to the platinum centre, can be described as having a twisted envelope type conformation with the E···E vector as the hinge. In **1** C(1), C(10) and C(9) all lie in a plane with S(1) lying 0.525(1) Å below the plane and S(2) lying 0.449(1) Å above the plane. This results in a non-planar, twisted PtS_2C_3 ring. In **6** the $PtSe_2C_3$ ring is close to planar with the selenium atoms deviating from the plane by 0.012-0.019(1) Å. The mean plane of E(1), E(2), C(1), C(10) and C(9) and the displacement of Pt(1), which sits in the *peri*-gap above the plane, is measured. In **1** the Pt(1) sits 0.937(1) Å above the mean plane and the angle of the S(1)···S(2) hinge is 144.13(1)°. Whereas in **6** the Pt(1) sits 1.037(1) Å above the mean plane and the Se(1)···Se(2) hinge angle is 142.98(1)°.

Unfortunately during our previous investigations the molecular structure of $[Pt(NapS_2)(PPh_3)_2]$[10] could not be obtained and therefore a comparison of the different *peri*-dithiolate backbones and their effect on the platinum metal geometry cannot be discussed. However, molecular structures were obtained for the selenium complexes; $[Pt(NapSe_2)(PPh_3)_2]$,[10] $[Pt(AcenapSe_2)(PPh_3)_2]$[11] and **6**, allowing a direct comparison between backbones to me

made. [Pt(NapSe$_2$)(PPh$_3$)$_2$][10] crystallises with two molecules in the asymmetric unit and one molecule of dichloromethane; [Pt(AcenapSe$_2$)(PPh$_3$)$_2$][11] and **6** crystallise as single molecules.

An increase in the non-bonded *peri*-distance is observed as the diselenolate ligand changes from naphthalene to acenaphthylene with values of 3.3721(9) Å, 3.437(3) Å and 3.452(4) Å for [Pt(NapSe$_2$)(PPh$_3$)$_2$], [Pt(AcenapSe$_2$)(PPh$_3$)$_2$] and **6**, respectively. This is accompanied by a steady increase in splay angle with values of 23.8°, 25.7° and 26.2°, respectively. This pattern is expected due to the addition of the ethane/ethene linker in acenaphthene/acenaphthylene causing the C(4)-C(5)-C(6) angle to decrease from 118.64(1)° in [Pt(NapSe$_2$)(PPh$_3$)$_2$] to *ca*. 109° in [Pt(AcenapSe$_2$)(PPh$_3$)$_2$] and **6**. A decrease in this angle at the bottom of the ring causes an increase in the angles of the splay region which consequently leads to an increase in *peri*-distance. A decrease in out-of-plane distortion occurs with [Pt(NapSe$_2$)(PPh$_3$)$_2$] displaying the greatest out-of-plane displacement with one selenium atom lying 0.234(1) Å above the naphthyl plane and one 0.165(1) Å below. [Pt(NapSe$_2$)(PPh$_3$)$_2$] also has the largest deformation of the naphthalene scaffold with torsion angles varying from the 'ideal' 180° by 1.1-2.4°. The naphthalene complex has the largest out-of-plane distortion and deformation of the backbone due to the absence of the ethane/ethene linker in the backbone which allows the system more flexibility.

The platinum metal adopts a distorted square planar geometry in all three complexes, with **6** displaying the most regular geometry. A steady increase in the Se(1)-Pt(1)-Se(2) angle is observed with values of 87.36(2)°, 89.27(6)° and 90.12(8)° for [Pt(NapSe$_2$)(PPh$_3$)$_2$], [Pt(AcenapSe$_2$)(PPh$_3$)$_2$] and **6**, respectively. This increase is a direct consequence of the increasing splay angle which is caused by the compression of the C(4)-C(5)-C(6) angle. As the Se(1)-Pt(1)-Se(2) angle increases, and therefore becomes closer to the ideal '90°', the P(1)-Pt(1)-P(2) angle decreases with values of 98.40(6)°, 97.68(13)° and 96.98(11)° for [Pt(NapSe$_2$)(PPh$_3$)$_2$], [Pt(AcenapSe$_2$)(PPh$_3$)$_2$] and **6**, respectively. No significant differences occur between the P-Pt-Se angles with values in the range of 86.5-88.3°. There are no differences observed in the Pt bond lengths between complexes. However, within the complexes the Pt(1)-Se bonds are longer (*ca.* 2.43-2.45 Å) than the Pt(1)-P bonds (*ca.* 2.28-2.30 Å).

Conclusions

The work presented in this paper builds on our previous studies of platinum *bis*phosphine complexes bearing dichalcogenate based ligands.[11] Herein we present the synthesis of a related series of platinum complexes **1**-**4** and **6**-**8** prepared from acenaphtho[5,6-cd]-1,2-dichalcogenoles [AcenapylE$_2$] **L1** (E = S) and **L2** (E = Se) and *cis*-[PtCl$_2$(PR$_3$)$_2$] (R$_3$ = Ph$_3$, Ph$_2$Me, PhMe$_2$, Me$_3$). For their synthesis, the appropriate disulfide or diselenide species was treated with lithium triethylborohydride resulting in *in situ* reduction of the AcenapylE$_2$ E-E bond to form the corresponding dilithio-species. Subsequent metathetical addition to a suspension of the *cis*-[PtCl$_2$(PR$_3$)$_2$] in THF afforded the respective platinum(II) complexes [Pt(5,6-AcenapylE$_2$)(PR$_3$)$_2$] (**1** E = S, R$_3$ = Ph$_3$; **2** E = S, R$_3$ = Ph$_2$Me; **3** E = S, R$_3$ = PhMe$_2$; **4** E = S, R$_3$ = Me$_3$; **6** E = Se, R$_3$ = Ph$_3$; **7** E = Se, R$_3$ = Ph$_2$Me; **8** E = Se, R$_3$ = PhMe$_2$). In a similar reaction, the dilithio-species of **L1** and **L2** were also reacted with (1,5-cyclooctadiene)platinum(II) dichloride; this led to only the formation of the **L1** platinum complex [Pt(5,6-AcenapylS$_2$)(COD)] (**5**).

^{31}P{^{1}H} NMR spectra of the sulfur complexes, **1**-**4**, display the expected single resonances with platinum satellites, moving to lower chemical shifts and with decreasing $^1J(^{31}\text{P}\text{-}^{195}\text{Pt})$ coupling constants as the alkyl group on phosphorus

is varied from R_3 = Ph_3 to R_3=Me_3. In complexes **6-8**, the addition of the low abundant ^{77}Se NMR active isotope provides extra complexity to their respective $^{31}P\{^1H\}$ and ^{77}Se NMR spectra. Secondary isotopomer effects cause the two ^{31}P atoms to align with either a *cis* or *trans* configuration with respect to the ^{77}Se NMR active isotope, making them magnetically inequivalent and creating a complex satellite system.

The X-ray structure for the known compound **L1** was investigated as no crystal data have been published.[3] It was found that **L1** displays similar characteristics to naphtha[1,8-*cd*][1,2]dithiole [$NapS_2$][10] and 5,6-dihydroacenaphtho[5,6-*cd*]-1,2-dithiole [$AcenapS_2$].[11] All three ligands were found to have statistically equivalent *peri*-distances and similar degrees of out-of-plane displacement and splay angle magnitude. **L1** showed the largest, although still minor, deviation from the ideal 180° C-C-C-C torsion angles by 1.88° and 2.20°. X-ray structures determined for **1**, **3** and **6** were analysed by platinum metal geometry, *peri*-atom displacement, splay angle magnitude, acenaphthylene ring torsion angles and E···E interactions. In each complex the acenaphtho[5,6-*cd*]-1,2-dichalcogenate ligand coordinates in a bidentate fashion to the platinum metal to form a six-membered PtE_2C_3 ring that can be described as having a twisted envelope type conformation. The platinum metal adopts a distorted square planar environment with angles deviating from the ideal 90°. Naturally, there is a significant increase in molecular distortion of the acenaphthylene ring system due to breaking of the chalcogen-chalcogen bond and insertion of the platinum. Complex **1** was found to have the greatest molecular distortion of all three complexes, showing that changing the phosphine group and also the chalcogen has a noticeable effect. Comparisons were made between **6** and our previously reported [Pt($NapSe_2$)(PPh_3)$_2$] and [Pt($AcenapSe_2$)(PPh_3)$_2$] complexes; the level of distortion was found to decrease as the backbone is altered from naphthalene to acenaphthylene.

Experimental Section

All experiments were carried out under an oxygen- and moisture-free nitrogen atmosphere using standard Schlenk techniques and glassware. Reagents were obtained from commercial sources and used as received. Dry solvents were collected from a MBraun solvent system. Elemental analyses were performed by Stephen Boyer at the London Metropolitan University. Infra-red spectra were recorded for solids as KBr discs in the range 4000-350 cm^{-1} on a Perkin-Elmer System 2000 Fourier transform spectrometer. ^{1}H, ^{13}C, ^{31}P and ^{77}Se NMR were recorded on a Jeol GSX 270 MHz spectrometer with δ(H) and δ(C) referenced to external tetramethylsilane, δ(P) referenced to external phosphoric acid and δ(Se) referenced to external dimethyl diselenide. Assignments of ^{13}C and ^{1}H NMR spectra were made with the help of H-H COSY and HSQC experiments. All measurements were performed at 25 °C. All values reported for NMR spectroscopy are in parts per million (ppm). Coupling constants (*J*) are given in Hertz (Hz). Mass spectrometry was performed by the University of St. Andrews Mass Spectrometry Service. Electrospray Mass Spectrometry (ESMS) was carried out on a Micromass LCT orthogonal accelerator time of flight mass spectrometer. All *cis*-dichloro*bis*(phosphine)platinum reagents were prepared following standard literature procedures.[20,21,22] 5,6-Dibromoacenaphthylene was also prepared following literature procedure.[13]

Acenaphtho[5,6-*cd*][1,2]dithiole [$AcenapylS_2$] (L1): TMEDA (5.8 mL, 38.4 mmol) was added in one portion to a solution of 5,6-dibromoacenaphthylene (5.95 g, 19.2 mmol) in diethyl ether (250 mL). The reaction was cooled to -78 °C and stirred for 15 min. A 2.5 M hexane solution of *n*-butyllithium (7.7 mL, 19.2 mmol) was added dropwise and the mixture was stirred for 15 min. Sulfur powder (0.62 g, 19.3 mmol) was added and the mixture was stirred at -40 °C for 2 h. The mixture was cooled again to -78 °C and a 2.5 M hexane solution of *n*-butyllithium (7.7 mL, 19.2 mmol) was

added dropwise and the mixture was stirred for 15 min. Sulfur powder (0.62 g, 19.3 mmol) was added and the mixture was stirred at -40 °C for a further 2 h. The mixture was then warmed to room temperature, quenched with acetic acid (2 mL) and exposed to an air stream overnight for mild oxidation. The resulting solution was evaporated under reduced pressure and then water (200 mL) was added and the mixture was extracted with dichloromethane (4 x 200 mL). The extract was dried with anhydrous magnesium sulfate and concentrated under reduced pressure to give a deep red oil. The oil was dissolved in hexane (100 mL) and refluxed for an hour. The hot solution was placed in the freezer at - 30 °C overnight to yield an orange solid (0.22 g, 5%); mp 166-168 °C; elemental analysis(Found: C, 67.1; H, 2.7. Calc. for $C_{12}H_6S_2$: C, 67.25; H, 2.8%); IR (KBr disc) ν_{max} cm^{-1} 3423w, 3035w, 2953s, 2924s, 2856s, 1596s, 1487w, 1462s, 1413vs, 1396vs, 1371vs, 1195w, 1108w, 1077s, 1025s, 823vs, 732w, 645w, 529w, 388w; ^{1}H NMR ($CDCl_3$, Me_4Si, 270 MHz) δ_H 7.88 (2 H, d, $^3J_{HH}$ 7.5 Hz, Acenapyl 4,7-H), 7.54 (2 H, d, $^3J_{HH}$ 7.7 Hz, Acenapyl 3,8-H), 7.25 (2 H, s, Acenapyl 9,10-H); ^{13}C{^{1}H} NMR ($CDCl_3$, Me_4Si, 76 MHz) δ_C 126.2(s), 126.0(s), 116.5(s); MS (ES^+): *m/z* 215.00 (30%, M^+).

Acenaphtho[5,6-*cd*][1,2]diselenole [AcenapylSe_2] (L2): Ligand **L2** was prepared following a similar procedure to that described for **L1** using 5,6-dibromoacenaphthylene (2.27 g, 7.34 mmol), TMEDA (2.2 mL, 14.7 mmol), a 2.5 M hexane solution of *n*-butyllithium (5.9 mL, 14.7 mmol) and selenium powder (1.16 g, 14.7 mmol) to yield a dark orange-brown solid (0.58 g, 26%; mp 147-149 °C (decomp.); elemental analysis (Found: C, 46.7; H, 2.0. Calc. for $C_{12}H_6Se_2$: C, 46.8; H, 2.0%); IR (KBr disc) ν_{max} cm^{-1} 2921w, 2366w, 2344w, 1596w, 1463w, 1400vs, 1213w, 1079s, 1020s, 822vs, 793s, 726w, 639s, 496w; ^{1}H NMR ($CDCl_3$, Me_4Si, 270 MHz) δ_H 7.76 (2 H, d, $^3J_{HH}$ 7.5 Hz, Acenapyl 4,7-H), 7.66 (2 H, d, $^3J_{HH}$ 7.7 Hz, Acenapyl 3,8-H), 7.17 (2 H, s, Acenapyl 9,10-H); ^{13}C{^{1}H} NMR ($CDCl_3$, Me_4Si, 76 MHz) δ_C 126.3(s), 125.8(s), 121.4(s); δ_{Se} (51.5 MHz; $CDCl_3$; 25 °C; MeSeSeMe) 542.7 (s); MS (ES^+): *m/z* 310.89 (100%, M^+).

[Pt(PPh_3)$_2$L1] (1): Lithium triethylborohydride (0.95 mL of a 1.0 M solution in THF, 0.95 mmol) was added to a solution of acenaphtho[5,6-*cd*][1,2]dithiole (0.10 g, 0.47 mmol) in THF (20 mL). An immediate colour change occurred from orange to deep red, along with the evolution of gas. After stirring for 30 min, the resulting solution was transferred *via* a stainless steel cannula to a suspension of *cis*-dichloro*bis*(triphenylphosphine)platinum (0.38 g, 0.47 mmol) in THF (10 mL). The mixture was stirred for 24 h resulting in a red solution. The solution was poured through a shallow pad of silica and eluted with dichloromethane (100 mL). The filtrate was evaporated to dryness under reduced pressure and redissolved in dichloromethane (10 mL). Slow addition of a mixture of diethyl ether (25 mL) and hexane (75 mL) resulted in precipitation of a dark red solid, which was collected and dried *in vacuo*; (0.10 g, 23%); mp 227-229 °C (decomp.); elemental analysis (Found: C, 57.9; H, 3.7. Calc. for $C_{48}H_{36}P_2PtS_2$.1.5 x CH_2Cl_2: C, 57.8; H, 3.8%); IR (KBr disc) ν_{max} cm^{-1} 3051w, 2361w, 1579s, 1479s, 1433vs, 1400vs, 1333s, 1309s, 1184w, 1115s, 1097vs, 1073vs, 1032vs, 998s, 828s, 737s, 691vs, 653s, 540vs, 521vs, 509vs, 495vs, 457w, 420w; ^{1}H NMR ($CDCl_3$, Me_4Si, 270 MHz) δ_H 7.62-7.44 (14 H, m, Acenapyl 4,7-H, P-Phenyl), 7.42-7.30 (6 H, m, P-Phenyl), 7.28 (2 H, d, $^3J_{HH}$ 5.3 Hz, Acenapyl 3,8-H), 7.26-7.13 (12 H, m, P-Phenyl), 6.85 (2 H, s, Acenapyl 9,10-H); ^{13}C{^{1}H} NMR ($CDCl_3$, Me_4Si, 76 MHz) δ_C 135.9-135.2(m), 130.8(s), 128.5-127.9(m), 126.9-126.7(m), 125.3(s), 124.4(s); ^{31}P{^{1}H} NMR ($CDCl_3$, H_3PO_4, 203 MHz) δ_P 23.9 (s, $^1J_{PPt}$ 2953 Hz); MS (ES^+): *m/z* 934.14 (28%, M^+).

[Pt(PPh_2Me)$_2$L1] (2): Complex **2** was prepared following a similar procedure to that described for **1** using acenaphtho[5,6-*cd*][1,2]dithiole (0.11 g, 0.49 mmol), lithium triethylborohydride (0.95 mL of a 1.0 M solution in THF, 0.95 mmol), and *cis*- dichloro*bis*(diphenylmethylphosphine)platinum (0.32 g, 0.49 mmol) to yield an orange solid (0.17 g, 42%); mp 117-119 °C (decomp.); elemental analysis (Found: C, 54.4; H, 3.8. Calc. for $C_{38}H_{32}PtP_2S_2$.1/2CH_2Cl_2: C,

54.3; H, 3.9%); IR (KBr disc) ν_{max} cm^{-1} 3424w, 3053w, 2922w, 2363s, 2342w, 1576w, 1463w, 1436s, 1402vs, 1332s, 1310w, 1180w, 1102s, 1072s, 1035s, 890vs, 830w, 736s, 693s, 510s, 452w; ^{1}H NMR ($CDCl_3$, Me_4Si, 270 MHz) δ_H 7.52 (2 H, d, $^{3}J_{HH}$ 7.4 Hz, Acenapyl 4,7-H), 7.49-7.42 (8 H, m, P-Phenyl), 7.38-7.28 (4 H, m, P-Phenyl), 7.28-7.18 (8 H, m, P-Phenyl), 7.11-7.04 (2 H, m, Acenapyl 3,8-H), 6.80 (2 H, s, Acenapyl 9,10-H), 1.83 (6 H, d, $^{1}J_{PH}$ 9.4 Hz); $^{13}C\{^{1}H\}$ NMR ($CDCl_3$, Me_4Si, 76 MHz) δ_C 133.6-133.5(m), 131.1(s), 128.8-128.6(m), 126.7(s), 125.0(s), 124.4(s), 14.6 (d, $^{1}J_{CP}$ 41 Hz); $^{31}P\{^{1}H\}$ NMR ($CDCl_3$, H_3PO_4, 203 MHz) δ_P 3.5 (s, $^{1}J_{PPt}$ 2880 Hz); MS (ES^+): *m/z* 796.20 (100%, M^+ - Me).

[Pt(PPhMe$_2$)$_2$L1] (3): Complex **3** was prepared following a similar procedure to that described for **1** using acenaphtho[5,6-*cd*][1,2]dithiole (0.11 g, 0.51 mmol), lithium triethylborohydride (0.95 mL of a 1.0 M solution in THF, 0.95 mmol), and *cis*- dichloro*bis*(dimethylphenylphosphine)platinum (0.26 g, 0.48 mmol) to yield an orange solid (0.09 g, 27%); mp 68-70 °C (decomp.); elemental analysis (Found: C, 48.95; H, 4.0. Calc. for $C_{28}H_{28}PtP_2S_2$: C, 49.05; H, 4.1%); IR (KBr disc) ν_{max} cm^{-1} 3425w, 2913w, 1577s, 1462w, 1435s, 1402vs, 1332w, 1308w, 1176w, 1107s, 1072s, 948s, 911vs, 836vs, 744s, 716w, 694s, 654w, 533w, 488w, 444w; ^{1}H NMR ($CDCl_3$, Me_4Si, 270 MHz) δ_H 7.82 (2 H, d, $^{3}J_{HH}$ 7.5 Hz, Acenapyl 4,7-H), 7.45-7.36 (4 H, m, P-Phenyl), 7.39 (2 H, d, $^{3}J_{HH}$ 7.5 Hz, Acenapyl 3,8-H), 7.35-7.27 (2 H, m, P-Phenyl), 7.26-7.17 (4 H, m, P-Phenyl), 6.87 (2 H, s, Acenapyl 9,10-H), 1.62 (12 H, d, $^{1}J_{PH}$ 10.0 Hz); $^{13}C\{^{1}H\}$ NMR ($CDCl_3$, Me_4Si, 76 MHz) δ_C 131.8-131.4(m), 129.4(br s), 129.1-129.0(m), 126.7(s), 124.8(s), 124.4(s), 13.7 (d, $^{1}J_{CP}$ 40 Hz) ; $^{31}P\{^{1}H\}$ NMR ($CDCl_3$, H_3PO_4, 203 MHz) δ_P -14.5 (s, $^{1}J_{PPt}$ 2819 Hz); MS (ES^+): *m/z* 578.08 (100%, M^+ - $PhMe_2$).

[Pt(PMe$_3$)$_2$L1] (4): Complex **4** was prepared following a similar procedure to that described for **1** using acenaphtho[5,6-*cd*][1,2]dithiole (0.10 g, 0.48 mmol), lithium triethylborohydride (0.95 mL of a 1.0 M solution in THF, 0.95 mmol), and *cis*-dichloro*bis*(trimethylphosphine)platinum (0.20 g, 0.48 mmol) to yield an impure brown solid; $^{31}P\{^{1}H\}$ NMR ($CDCl_3$, H_3PO_4, 203 MHz) δ_P -24.7 (s, $^{1}J_{PPt}$ 2768 Hz).

[Pt(COD)L1] (5): Complex **5** was prepared following a similar procedure to that described for **1** using acenaphtho[5,6-*cd*][1,2]dithiole (0.10 g, 0.47 mmol), lithium triethylborohydride (0.95 mL of a 1.0 M solution in THF, 0.95 mmol), and (1,5-cyclooctadiene)platinum(II) dichloride (0.18 g, 0.47 mmol) to yield an orange solid (0.04 g, 14%); mp >300 °C; elemental analysis (Found: C, 46.3; H, 3.6. Calc. for $C_{20}H_{18}PtS_2$: C, 46.4; H, 3.5%); IR (KBr disc) ν_{max} cm^{-1} 2923s, 2872s, 2363s, 2343w, 1580w, 1462w, 1408vs, 1335w, 1261s, 1179w, 1073vs, 1034vs, 831s, 800s, 729w, 651w, 535w; ^{1}H NMR ($CDCl_3$, Me_4Si, 270 MHz) δ_H 7.73 (2 H, d, $^{3}J_{HH}$ 7.5 Hz, Acenapyl 4,7-H), 7.48 (2 H, d, $^{3}J_{HH}$ 7.5 Hz, Acenapyl 3,8-H), 6.97 (2 H, s, Acenapyl 9,10-H), 5.18 (4 H, s, COD-CH_2), 2.71-2.59 (4 H, m, COD-CH_2), 2.55-2.34 (4 H, m, COD-CH_2); $^{13}C\{^{1}H\}$ NMR ($CDCl_3$, Me_4Si, 76 MHz) δ_C 125.6(s), 125.3(s), 124.6(s), 100.6(s), 30.7(s); MS (ES^+): *m/z* 518.06 (100%, M^+ + H).

[Pt(PPh$_3$)$_2$L2] (6): Complex **6** was prepared following a similar procedure to that described for **1** using acenaphtho[5,6-*cd*][1,2]diselenole (0.10 g, 0.34 mmol), lithium triethylborohydride (0.65 mL of a 1.0 M solution in THF, 0.65 mmol), and *cis*- dichloro*bis*(triphenylphosphine)platinum (0.26 g, 0.33 mmol) to yield a red solid (0.16 g, 48%); mp 159-161 °C; elemental analysis (Found: C, 55.9; H, 3.6. Calc. for $C_{48}H_{36}PtP_2Se_2$: C, 56.1; H, 3.5%); IR (KBr disc) ν_{max} cm^{-1} 3408w, 3052w, 2925w, 1581w, 1479s, 1435vs, 1400vs, 1331s, 1185w, 1159w, 1094vs, 1073s, 1026s, 1000w, 831w, 743s, 693vs, 646w, 539vs, 522vs, 496s, 459w, 422w; ^{1}H NMR ($CDCl_3$, Me_4Si, 270 MHz) δ_H 7.70 (2 H, d, $^{3}J_{HH}$ 7.3 Hz, Acenapyl 4,7-H), 7.60-7.48 (12 H, m, P-Phenyl), 7.39-7.27 (8 H, m, Acenapyl 3, 8-H, P-Phenyl), 7.25-7.12 (12 H, m,

P-Phenyl), 6.85 (2 H, s, Acenapyl 9,10-H); $^{13}C\{^1H\}$ NMR ($CDCl_3$, Me_4Si, 76 MHz) δ_C 135.8-135.0(m), 130.8(s), 129.7(br s), 128.3-127.8(m), 125.9(s), 124.2(s); $^{31}P\{^1H\}$ NMR ($CDCl_3$, H_3PO_4, 203 MHz) δ_P 20.2 (s, $^1J_{PPt}$ 3014 Hz); $^{77}Se\{^1H\}$ NMR ($CDCl_3$, Me_2Se_2, 51.5 MHz) δ_{Se} 227.6 (pseudo-triplet,^{1} $^2J_{SeP}$ 55 Hz, $^1J_{SePt}$ 178 Hz); MS (ES^+): *m/z* 1028.03 (100%, M^+ + H).

[Pt(PPh$_2$Me)$_2$L2] (7): Complex **7** was prepared following a similar procedure to that described for **1** using acenaphtho[5,6-*cd*][1,2]diselenole (0.10 g, 0.33 mmol), lithium triethylborohydride (0.66 mL of a 1.0 M solution in THF, 0.66 mmol), and *cis*- dichloro*bis*(diphenylmethylphosphine)platinum (0.21 g, 0.32 mmol) to yield a red solid (0.07 g, 25%); mp 116-118 °C; elemental analysis (Found: C, 50.4; H, 3.7. Calc. for $C_{38}H_{32}PtP_2Se_2$: C, 50.5; H, 3.6%); IR (KBr disc) ν_{max} cm^{-1} 3422w, 3051w, 2922w, 2361s, 2343w, 1579s, 1561w, 1475s, 1435vs, 1399vs, 1330s, 1182w, 1101s, 1072s, 1026s, 999w, 889vs, 831s, 734s, 693vs, 647w, 509s, 490s, 451s; ^1H NMR ($CDCl_3$, Me_4Si, 270 MHz) δ_H 7.87 (2 H, d, $^3J_{HH}$ 7.3 Hz, Acenapyl 4,7-H), 7.49-7.38 (8 H, m, P-Phenyl), 7.49-7.38 (4 H, m, P-Phenyl), 7.38-7.29 (8 H, m, P-Phenyl), 7.25 (2 H, d, $^3J_{HH}$ 7.4 Hz, Acenapyl 3,8-H), 6.85 (2 H, s, Acenapyl 9,10-H), 1.91 (6 H, d, $^1J_{PH}$ 8.9 Hz); $^{13}C\{^1H\}$ NMR ($CDCl_3$, Me_4Si, 76 MHz) δ_C 133.5 (d, $^2J_{CP}$ 6.8 Hz), 131.8(s), 129.7 (d, $^4J_{CP}$ 4.3 Hz), 128.7 (d, $^3J_{CP}$ 4.9 Hz), 125.9(s), 124.2(s), 15.5 (br s); $^{31}P\{^1H\}$ NMR ($CDCl_3$, H_3PO_4, 203 MHz) δ_P 0.6 (s, $^1J_{PPt}$ 2932 Hz); $^{77}Se\{^1H\}$ NMR ($CDCl_3$, Me_2Se_2, 51.5 MHz) δ_{Se} 204.5 (pseudo-triplet,^{1} $^2J_{SeP}$ 55 Hz, $^1J_{SePt}$ 210 Hz); MS (ES^+): *m/z* 750.06 (45%, M^+ - Ph_2).

[Pt(PPhMe$_2$)$_2$L2] (8): Complex **8** was prepared following a similar procedure to that described for **1** using acenaphtho[5,6-*cd*][1,2]diselenole (0.10 g, 0.34 mmol), lithium triethylborohydride (0.65 mL of a 1.0 M solution in THF, 0.65 mmol), and *cis*- dichloro*bis*(dimethylphenylphosphine)platinum (0.18 g, 0.33 mmol) to yield a red solid (0.06 g, 22%); mp 66-68 °C (decomp.); IR (KBr disc) ν_{max} cm^{-1} 3423vs, 3050w, 2908w, 2361w, 2344w, 1638w, 1579s, 1561w, 1467w, 1435s, 1398vs, 1329s, 1312w, 1283w, 1181w, 1105s, 1072s, 1027s, 1000w, 1105s, 1072s, 1027s, 946vs, 908vs, 834s, 743s, 714s, 694s, 647s, 489s, 443s, 371w; ^1H NMR ($CDCl_3$, Me_4Si, 270 MHz) δ_H 8.14 (2 H, d, $^3J_{HH}$ 7.2 Hz, Acenapyl 4,7-H), 7.62-7.49 (4 H, m, P-Phenyl), 7.50-7.30 (8 H, m, P-Phenyl, Acenapyl 3,8-H), 6.92 (2 H, s, Acenapyl 9,10-H), 1.72 (12 H, d, $^1J_{PH}$ 9.7 Hz); $^{13}C\{^1H\}$ NMR ($CDCl_3$, Me_4Si, 76 MHz) δ_C 131.5-131.1(m), 129.8(s), 129.5(br s), 129.1-128.9(m), 125.8(s), 124.3(s), 14.5 (d, $^1J_{CP}$ 40 Hz); $^{31}P\{^1H\}$ NMR ($CDCl_3$, H_3PO_4, 203 MHz) δ_P -17.6 (s, $^1J_{PPt}$ 2873 Hz, $^2J_{PSe}$ 52 Hz); $^{77}Se\{^1H\}$ NMR ($CDCl_3$, Me_2Se_2, 51.5 MHz) δ_{Se} 174.6 (pseudo triplet,^{1} $^2J_{SeP}$ 53 Hz, $^1J_{SePt}$ 251 Hz); MS (ES^+): *m/z* 786.04 (60%, M^+ + Li).

Crystal Structure Analyses

X-ray crystal structures for **L1** and **3** were determined at -100(1) °C and -180(1) °C, respectively, using a Rigaku XtaLAB P200 diffractometer (Mo Kα radiation, confocal optic). Intensities were corrected for Lorentz, polarisation and absorption. Data for compound **1** were collected at -180(1) °C by using a Rigaku MM007 High brilliance RA generator (Mo Kα radiation, confocal optic) and Saturn CCD system. At least a full hemisphere of data was collected using ω scans. Intensities were corrected for Lorentz, polarisation and absorption. Data for compound **6** were collected at -100(1) °C on a Rigaku SCXmini CCD area detector with graphite-monochromated Mo-Kα radiation (λ = 0.71073 Å). The data were corrected for Lorentz, polarisation and absorption. Data for all compounds analyzed were collected and processed using CrystalClear (Rigaku).[23] Structures were solved by direct methods[24] and expanded using Fourier techniques.[25] Non-hydrogen atoms were refined anisotropically. Hydrogen atoms were refined using the riding model. All calculations were performed using the CrystalStructure[26] crystallographic software package except for

refinement, which was performed using SHELXL2013.[27] All images of molecular structures were generated using OLEX2.[28]

Table 4. Crystallographic data for compounds **L1**, **1**, **3**, and **6**.

Compound	**L1**	**1**	**3**	**6**
Empirical Formula	$C_{12}H_6S_2$	$C_{49.5}H_{39}Cl_3P_2PtS_2$	$C_{28}H_{28}P_2PtS_2$	$C_{48}H_{36}P_2PtSe_2$
Formula Weight	214.30	1061.37	685.69	1027.77
Temperature (°C)	-100.0	-180.0	-180.0	-100.0
Crystal Colour, Habit	orange, chip	red, prism	orange, prism	red, prism
Crystal Dimensions (mm^3)	0.090 X 0.050 X 0.020	0.100 X 0.100 X 0.100	0.100 X 0.100 X 0.020	0.129 X 0.122 X 0.079
Crystal System	monoclinic	orthorhombic	monoclinic	monoclinic
Lattice Parameters	a = 7.4390(19) Å	a = 21.978(4) Å	a = 15.708(4) Å	a = 9.943(11) Å
	b = 11.323(3) Å	b = 58.311(10) Å	b = 9.991(2) Å	b = 17.589(18) Å
	c = 11.165(3) Å	c = 13.808(3) Å	c = 16.400(4) Å	c = 22.95(2) Å
	-	-	-	-
	β = 105.277(5)°	-	β = 93.805(5)°	β = 101.467(10)°
	-	-	-	-
Volume ($Å^3$)	907.2(4)	17696(6)	2567.9(11)	3933(7)
Space Group	$P2_1/c$	Fdd2	$P2_1/c$	$P2_1/n$
Z Value	4	16	4	4
Dcalc (g/cm^3)	1.608	1.593	1.773	1.735
F000	440	8432	1344	2000
μ(MoKα) (cm^{-1})	5.314	33.414	57.453	55.198
No. of Reflections Measured	10802	43690	33538	18295
Rint	0.0599	0.0549	0.1227	0.0902
Min and Max Transmissions	0.823 - 0.989	0.541 - 0.702	0.422 - 0.891	0.451- 0.647
Independ. Reflection (No. Variables)	1663(154)	8004(532)	4739(302)	7187(478)
Reflection/Parameter Ratio	10.80	15.05	15.69	15.04
Residuals: R1 (I>2.00σ(I))	0.0362	0.0407	0.1344	0.0536
Residuals: R (All Reflections)	0.0516	0.0415	0.1484	0.1124
Residuals: wR_2 (All Reflections)	0.0975	0.0979	0.3760	0.0836
Goodness of Fit Indicator	1.000	1.056	1.156	1.051
Maximum peak in Final Diff. Map	0.34 e-/$Å^3$	2.81 e-/$Å^3$	11.74 e-/$Å^3$	1.15 e-/$Å^3$
Minimum peak in Final Diff. Map	-0.24 e-/$Å^3$	-1.24 e^-/$Å^3$	-5.77 e^-/$Å^3$	-1.53 e^-/$Å^3$

CCDC <1005370-1005373 contains the supplementary crystallographic data for **L1, 1, 3** & **6**. These X-ray data can be obtained free of charge via www.ccdc.cam.ac.uk/conts/retrieving.html or from the Cambridge Crystallographic Data centre, 12 Union Road, Cambridge CB2 1EZ, UK; fax (+44) 1223-336-033; e-mail: deposit@ccdc.cam.ac.uk CCDC Nos:

Acknowledgments

Mass Spectrometry was performed at the University of St. Andrews Mass Spectrometry Service by Caroline Horsburgh. The work in this project was supported by the Engineering and Physical Sciences Research Council (EPSRC).

References

[1] a) C. A. Coulson, R. Daudel, J. M. Robertson, *Proc. R. Soc. London, Ser. A* **1951**, *207*, 306; b) D. W. Cruickshank, *Acta Crystallogr.* **1957**, *10*, 504; c) C. P. Brock, J. D. Dunitz, *Acta Crystallogr., Sect. B: Struct. Crystallogr. Cryst. Chem.* **1982**, *38*, 2218; d) J. Oddershede, S. Larsen, *J. Phys. Chem. A* **2004**, *108*, 1057.

[2] A. C. Hazell, R. G. Hazell, L. Norskov-Lauritsen, C. E. Briant, D. W. Jones, *Acta Crystallogr., Sect. C: Cryst. Struct. Commun.* **1986**, 42, 690.

[3] A. D. Rae, R. A. Wood, T. R. Welberry, *J. Chem. Soc., Perkin Trans. 2* **1985**, *3*, 451.

[4] A. Bondi, *J. Phys. Chem.* **1964**, *68*, 441.

[5] V. Balasubramaniyan, *Chem. Rev.* **1966**, *66*, 567.

[6] R. W. Alder, P. S. Bowman, W. R. S. Steele, D. R. Winterman, *Chem. Commun.* **1968**, 723; b) R. W. Alder, M. R. Bryce, N. C. Goode, N. Miller, J. Owen, *J. Chem. Soc., Perkin Trans. 1* **1981**, 2840; c) J. D. Hoefelmeyer, M. Schulte, M. Tschinkl, F. P. Gabbai, *Coord. Chem. Rev.* **2002**, *235*, 93; d) P. Kilian, F. R. Knight, J. D. Woollins, *Chem. Eur. J.* **2011**, *17*, 2302; e) P. Kilian, F. R. Knight, J. D. Woollins, *Coord. Chem. Rev.* **2011**, *255*, 1387.

[7] a) P. Wawrzyniak, A. M. Z. Slawin, A. L. Fuller, J. D. Woollins, P. Kilian, *Dalton Trans.* **2009**, *38*, 7883; b) V. V. Mezheritskii, A. N. Antonov, A. A. Milov, K. A. Lysenko, *Russ. J. Org. Chem.* **2010**, *46(6)*, 844; c) F. R. Knight, K. S. Athukorala Arachchige, R. A. M. Randall, M. Bühl, A. M. Z. Slawin, J. D. Woollins, *Dalton Trans.* **2012**, *41(11)*, 3154; d) M-L. Lechner, F. R. Knight, K. S. Athukorala Arachchige, R. A. M. Randall, M. Bühl, A. M. Z. Slawin, J. D. Woollins, *Organometallics* **2012**, *31*, 2922; e) L. A. Aschenbach, F. R. Knight, R. A. M. Randall, D. B. Cordes, A. Baggott, M. Bühl, A. M. Z. Slawin, J. D. Woollins, *Dalton Trans.* **2012**, *41*, 3141.f) M. W. Stanford, F. R. Knight, K. S. Athukorala Arachchige, P. Sanz Camacho, S. E. Ashbrook, M. Bühl, A. M. Z. Slawin, J. D. Woollins, *Dalton Trans*. **2014**, *43(17)*, 6548.

[8] a) G. P. Petrenko, E. N. Tel'nyuk, *Zh. Obshch. Khim*. **1966**, *2(4)*, 722; b) G. P. Petrenko, E. N. Tel'nyuk, *Zh. Org. Chim*. **1967**, *3(1)*, 180; c) G. P. Petrenko, E. N. Tel'nyuk., *Zh. Org. Khim*. **1967**, *3(5)*, 927; d) F. B. Mallory, C. W. Mallory, K. E. Butler, M. B. Lewis, A. Q. Xia, E. D. Luzik Jr., L. E. Fredenburgh, M. M. Ramanjulu, Q. N. Van, M. M. Francl, D. A. Freed, C. C. Wray, C. Hann, M. Nerz-Stormes, P. J. Carroll, L. E. Chirlian, *J. Am. Chem. Soc*. **2000**, *122*, 4108; e) V. A. Ozeryanskii, A. F. Pozharskii, G. R. Milgizina, S. T. Howard, *J. Org. Chem*. **2000**, *65*, 7707; f) A. N. Antonov, R. V. Tyurin, L. G. Minyaeva, V. V. Mezheritskii, *Russ. J. Org. Chem*. **2006**, *42(10)*, 1576.

[9] a) B. K. Teo, F. Wudl, J. H. Marshall, A. Krugger, *J. Am. Chem. Soc.* **1977**, *99*, 2349; b) B. K. Teo, P. A. Snyder-Robinson, *Inorg. Chem.* **1978**, *17*, 3489; c) B. K. Teo, P. A. Snyder-Robinson, *Inorg. Chem.* **1979**, *18*, 1490; d) B. K. Teo, P. A. Snyder-Robinson, *Inorg. Chem.* **1981**, *20*, 4235.

[10] S. M. Aucott, H. L. Milton, S. D. Robertson, A. M. Z. Slawin, G. D. Walker, J. D. Woollins, *Chem. Eur. J.* **2004**, *10*, 1666; S. D. Robertson, PhD Thesis, University of St Andrews (UK), **2005** and the references therein.

[11] C. G. M. Benson, C. M. Schofield, R. A. M. Randall, L. Wakefield, F. R. Knight, A. M. Z. Slawin, J. D. Woollins, *Eur. J. Inorg. Chem*. **2013**, 427.

[12] L-Y. Chiang and J. Meinwald, *Tetrahedron Lett*. **1980**, *21*, 4565.

[13] L. M. Diamond, F. R. Knight, K. S. Athukorala Arachchige, R. A. M. Randall, M. Bühl. A. M. Z. Slawin, J. D. Woollins, *Eur. J. Inorg. Chem*. **2014**, 9, 1512.

[14] R. V. Parish, *NMR, NQR, EPR, and Mössbauer Spectroscopy in Inorganic Chemistry*, Ellis Horwood Limited, Chichester England, 1990**.**

[15] C. P. Morley, C. A. Webster, P. Douglas, K. Rofe, M. Di Vaira, *Dalton Trans.* **2010**, *39*, 3177.

[16] a) G. Matsubayahi, A. Yokozawa, *Inorg. Chim. Acta*. **1993**, *208*, 95; b) V. C. Ginn, P. F. Kelly, J. D. Woollins, *Polyhedron* **1994**, *13(10)*, 1501; c) M. Risto, E. M. Jahr, M. S. Hannu-Kuure, R. Oilunkaniemi, R. S. Laitinen, *J. Organomet. Chem*. **2007**, *692*, 2193.

[17] J. A. Iggo (Ed.), *NMR Spectroscopy in Inorganic Chemistry*, Oxford University Press Inc., New York, **1999**.

[18] R. Steudel, Angew. *Chem. Int. Ed. Engl*. **1975**, *14(10)*, 655 and the references therein.

[19] W. H. Hersh, *J. Chem. Ed*. **1997**, *74*, 1485.

[20] D. Drew, J. R. Doyle, *Inorg. Synth*. **1972**, *13*, 47.

[21] F. J. Ramos-Lima, A. G. Quiroga, J. M. Pérez, M. Font-Bardía, X. Solans, C. Navarro-Ranninger, *Eur. J. Inorg. Chem.* **2003**, *8*, 1591.

[22] J. Bailar, H. Itatani, *Inorg. Chem.* **1965**, *4*, 1618.

[23] CrystalClear: Rigaku Corporation, 1999. CrystalClear Software User's Guide, Molecular Structure Corporation, (c) 2000. J. W. Pflugrath, *Acta Cryst*. 1999, **D55**, 1718-1725.

[24] SIR2004: M.C. Burla, R. Caliandro, M. Camalli, B. Carrozzini, G.L. Cascarano, L. De Caro, C. Giacovazzo, G. Polidori, R. Spagna, 2005.

[25] DIRDIF99: P. T. Beurskens, G. Admiraal, G. Beurskens, W. P. Bosman, R. de Gelder, R. Israel, J. M. M. Smits, 1999. The DIRDIF-99 program system, Technical Report of the Crystallography Laboratory, University of Nijmegen, The Netherlands.

[26] CrystalStructure 4.1: Crystal Structure Analysis Package, Rigaku Corporation (2000-2014). Tokyo 196-8666, Japan.

[27] SHELX2013: G. M. Sheldrick, 2013, University of Gottingen, Germany.

[28] OLEX2: O. V. Dolomanov, L. J. Bourhis, R. J. Gildea, J. A. K. Howard, H. Puschmann, *J. Appl. Cryst*. **2009**, *42*, 339.

TOC

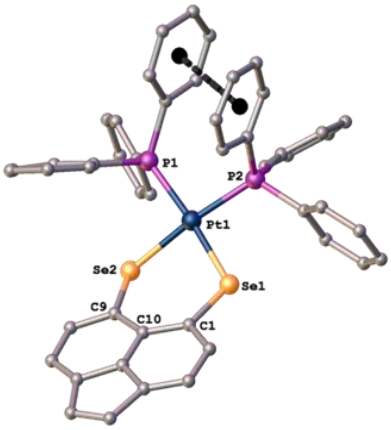

((Seven platinum *bis*phosphine complexes have been prepared from acenaphtho[5,6-*cd*]-1,2-dichalcogenoles AcenapylE_2 E = S, Se, following metathetical addition of the dilithium precursors to *cis*-[$PtCl_2(PR_3)_2$] (R_3 = Ph_3, Ph_2Me, $PhMe_2$, Me_3). [Pt(5,6-AcenapylS_2)(COD)] was also prepared in a similar manner from (1,5-cyclooctadiene)platinum(II) dichloride.))